

Millimeter-Wave Microstrip-Line-Fed Broadband Waveguide Aperture Antennas

Shintaro YANO[†], Student Member, Kunio SAKAKIBARA^{†a)}, Senior Member, Nobuyoshi KIKUMA[†], Fellow, and Hiroshi HIRAYAMA[†], Member

SUMMARY Microstrip-line-fed broadband aperture antennas were developed in the millimeter-wave band. We have developed broadband microstrip-to-waveguide transitions to connect a microstrip line and a waveguide. The waveguide transmission line was replaced by a radiating waveguide with an aperture to compose a microstrip-line-fed aperture antenna. Two types of aperture antennas were developed. First, the microstrip substrate is fixed between the two metal plates of a waveguide with an aperture and a back-short waveguide. Second, both the microstrip feeding-line and the back-short waveguide are accommodated in the two-layer LTCC substrate. Broadband performance was achieved due to the potential of the transition. The characteristics of the developed antennas were evaluated by simulations and experiments in the millimeter-wave band.

key words: Millimeter-Wave Antenna, Waveguide, LTCC substrate

1. Introduction

Millimeter-wave technologies have been expected to realize broadband high-speed wireless communication systems for home servers and HD video transmissions [1]–[3]. High-gain or beam-scanning antennas are required for base-station antennas. Mobile-station antennas should have properties of small size (lower gain), low loss and high integration with RF circuits. Many kinds of millimeter-wave antennas have been developed for wireless communication systems [4]–[11]. Multi-layer configuration such as LTCC (Low Temperature Co-fired Ceramics) substrates is one of the promising candidates for integration of an antenna into the RF circuits [4], [5], [11]. The RF module including an antenna is in a metal package for shielding from noises. The waveguide aperture is formed for wireless communication channels from the outside of the package. The microstrip-line-fed waveguide aperture antenna is attractive to connect the RF circuit directly to the waveguide aperture as shown in Fig. 1. Broad bandwidth is required to apply to the communication systems in the millimeter-wave band.

We have already developed two types of broadband microstrip-to-waveguide transitions to connect a microstrip line and a waveguide. One transition was composed of a microstrip substrate (Fluoro-carbon resin film, thickness $t = 0.127$ mm, relative dielectric constant $\epsilon_r = 2.2$ and loss tangent $\tan \delta = 0.001$) between the two metal plates of a waveguide transmission line and a back-short waveguide [12].

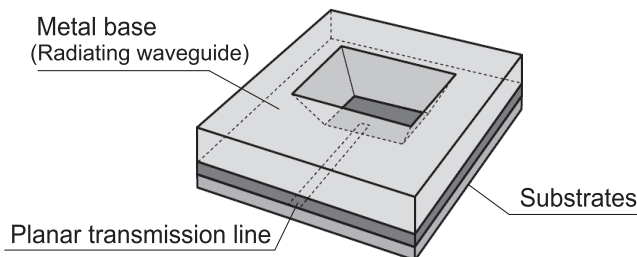


Fig. 1 Microstrip-line-fed waveguide aperture antenna on the millimeter-wave package.

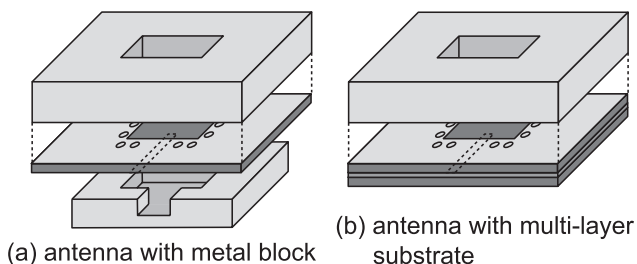


Fig. 2 Two types of the microstrip-line-fed waveguide aperture antenna.

Broad frequency bandwidth 30% for reflection lower than -15 dB was obtained although the metal block was necessary for back-short waveguide. The metal block for back-short waveguide was replaced by another dielectric substrate (Rogers RO4350B, thickness $t = 0.25$ mm, relative dielectric constant $\epsilon_r = 3.48$ and loss tangent $\tan \delta = 0.004$) to compose a multi-layer substrate in the other transition [13]. Although the bandwidth was narrower than the previous transition, the back-short waveguide was not necessary, which was good integration with RF circuit. The waveguide transmission lines of these transitions were replaced by the waveguide with the aperture to realize the waveguide aperture antennas in this work.

Two waveguide aperture antennas were developed by applying the two transitions as shown in Fig. 2. One is a waveguide aperture antenna with a metal block for the back-short waveguide and the other is the one with a multi-layer substrate. Broad bandwidth can be expected by using the former antenna due to the potential of the transition with a metal block for the back-short waveguide. Low profile, relatively broad bandwidth, and essentially no assembling error of the back-short quasi-waveguide on the substrate can be

Manuscript received March 7, 2011.

Manuscript revised July 7, 2011.

[†]The authors are with Nagoya Institute of Technology, Nagoya-shi, 466-8555 Japan.

a) E-mail: sakaki@nitech.ac.jp

DOI: 10.1587/transcom.E95.B.34

expected by using the antenna with a multi-layer substrate. The proposed antennas were developed by using the popular substrate for microwave circuit such as alumina and LTCC substrates with higher relative dielectric constant, while the transitions were developed by using the substrate with lower relative dielectric constant. The performances of the two waveguide aperture antennas were demonstrated by simulations and experiments in this paper.

2. Configuration of Waveguide Aperture Antennas

Two waveguide aperture antennas were developed in the millimeter-wave band. Both are formed by layer structures and have a waveguide with an aperture in the metal plate. One antenna consists of a single substrate with a back-short waveguide in another metal plate on the opposite plane of the substrate. The other antenna consists of a double-layer LTCC substrate. An additional metal plate is not necessary, because the back-short waveguide is in the substrate. The configurations of these antennas are indicated in the following sections.

2.1 Aperture Antenna with Metal Block for Back-Short Waveguide

The microstrip-line-fed waveguide aperture antenna with the metal block for the back-short waveguide was developed for broad frequency bandwidth. The configuration of the proposed antenna is shown in Fig. 3. The alumina substrate ($\epsilon_r = 9.8, \tan\delta = 0.0035$) with conductor patterns on its both sides is placed between the metal radiating waveguide (WR-10, $2.54 \times 1.27 \text{ mm}^2$) and the metal block for the back-short waveguide. The probe at the end of the microstrip line is inserted into the waveguide. Figure 4 indicates the cross-sectional view of the proposed antenna to show the principle of the transition. The microstrip line on BB'-plane is perpendicular to the waveguide axis. Via holes are surrounding the waveguide in the substrate to reduce leakage of parallel plate mode transmitting into the substrate. The short circuit at the end of the back-short waveguide is spaced by essentially $\lambda_g/4$ (λ_g : a guided wavelength of the waveguide) below the microstrip line. Consequently, electric current on the probe couples to magnetic field of TE₁₀ dominant mode of the radiating waveguide. Electromagnetic wave radiates from the aperture of the radiating waveguide. Arrows indicate electric field in the transition. The antenna performs mode transformation from the microstrip line to the waveguide and radiates electromagnetic wave from the aperture of the waveguide as shown in Fig. 4. The reflection from the waveguide aperture is also taken into consideration in the design.

Broad bandwidth is an advantage for the aperture antennas with the metal block. However, the additional parts of the metal block is required for the back-short waveguide and some degradation of the performance is observed due to the shift of the back-short waveguide from the waveguide center during assembling. The waveguide aperture antenna

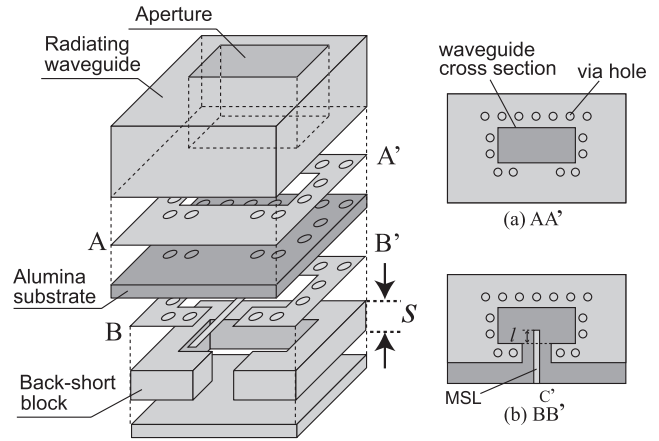


Fig. 3 Configuration of the aperture antenna with metal block for back-short waveguide.

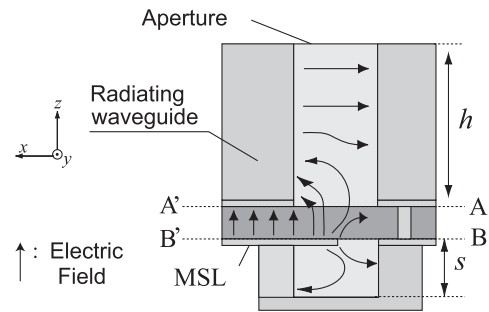


Fig. 4 Principle of the mode transformation for electric field in the antenna.

with multi-layer LTCC substrate is developed to avoid setting the metal block.

2.2 Aperture Antenna with Multi-Layer LTCC Substrate

The metal block for the back-short waveguide in the previous aperture antenna was replaced by the additional layer of the substrate. The aperture antenna is composed of the multi-layer LTCC substrate set on the waveguide with aperture, which results in low profile. The multi-layer LTCC substrate consists of two ceramics substrates ($\epsilon_r = 7.1, \tan\delta = 0.005$). Although the metal block is set carefully on the single substrate of the previous antenna, no assembling error is generated at the back-short waveguide of the multi-layer LTCC substrate.

The structure of the aperture antenna with multilayer substrate is shown in Figs. 5 and 6. The back-short quasi-waveguide is structured by surrounding via holes along the waveguide profile in the multi-layer substrate. Therefore, the thickness s of the substrate is identical to the length of the back-short waveguide of the antenna. The cut-off frequency is $1/\sqrt{\epsilon_r}$ times of that for the hollow waveguide, where ϵ_r is the relative dielectric constant of the substrate. Provided that the back-short waveguide with the same dimensions of the standard waveguide is structured in the substrate, unnecessary higher order mode is generated in the

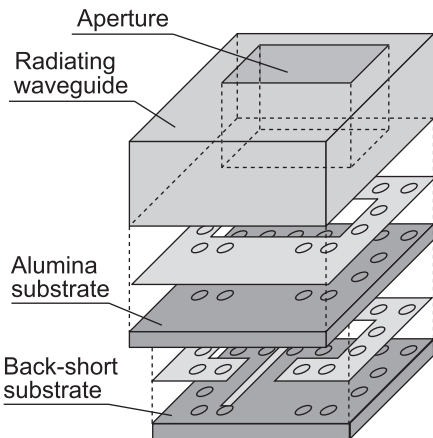


Fig. 5 Structure of the aperture antenna with multi-layer LTCC substrate.

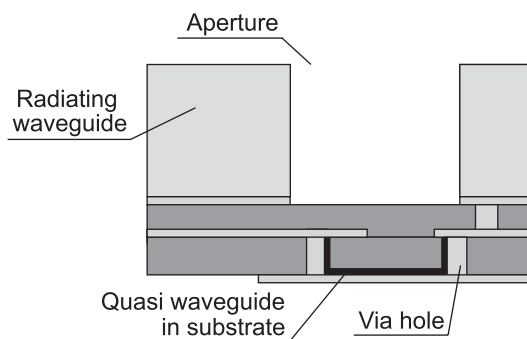


Fig. 6 Cross sectional view of the aperture antenna with multi-layer LTCC substrate to show the back-short waveguide in the substrate.

quasi-waveguide. The cut-off frequency can be controlled by the broad-wall width of the waveguide. The equivalent broad wall width

$$a' = \frac{a}{\sqrt{\epsilon_r}} \quad (1)$$

was used to prevent higher order mode. Moreover, taper structure of the printed pattern was supplied for matching at the connection between the feeding microstrip line and a grounded co-planar line around the input of the waveguide.

3. Simulations and Measurements

The proposed antennas were designed on the conditions of the dielectric constant, thickness of the commercially supplied substrates, and the minimum size of the via-hole diameters and printed patterns. The reflection S_{11} and directivity were calculated by using electromagnetic simulator Ansys HFSS of the finite element method. Measurements of S_{11} were carried out by using a probe station for microstrip line input. In this measurement, we adopt the calibration method to compensate the characteristics of the probe connections [14].

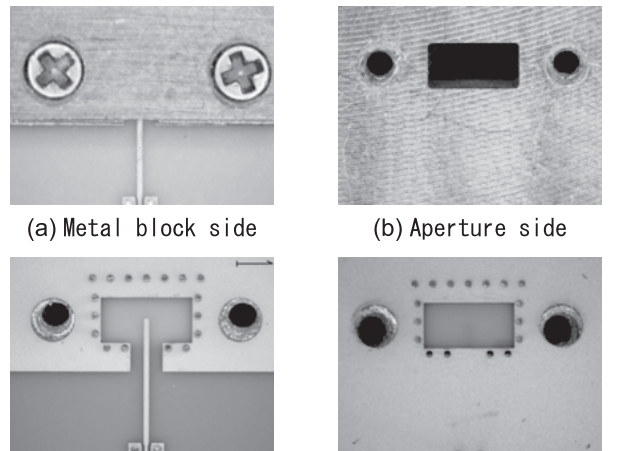


Fig. 7 Fabricated antenna with metal block for back-short waveguide.

3.1 Aperture Antenna with Metal Block for Back-Short Waveguide

Thickness t of the substrate is an important parameter and was chosen to be 0.15 mm from the limitation of the thickness variety of the commercially supplied substrates. The lengths l , s and h of the probe, the back-short waveguide, and the radiating waveguide, respectively, were optimized to operate broad frequency bandwidth. The proposed antenna was fabricated for measurement. Figure 7 shows photographs of the antenna. The metal plate with the aperture, the substrate, and the metal block with back-short waveguide were screwed together.

3.1.1 Reflection S_{11}

To demonstrate the dependency of the performance on the geometrical parameters for the antenna design, Figs. 8, 9 and 10 show the measured and simulated reflections S_{11} of the proposed antenna. The length h of the radiating waveguide, the back-short length s and the probe length l inserted into the waveguide are designed to be 4.3 mm, 0.4 mm and 0.68 mm, respectively. Double resonance is observed in both simulation and measurement, which causes wide bandwidth. Bandwidth of the reflection lower than -10 dB is broad and is 12.8 GHz (16.7%) because of the double resonance as indicated by the thin solid line in Fig. 8.

Figure 8 shows the reflection S_{11} in changing the back-short length s , where the length h of the radiating waveguide is fixed to 4.3 mm. In this case, only higher resonant frequency shifts toward lower when s increases. Although the simulated lower resonant frequency almost agrees well with the measured one, the measured higher resonant frequency for $s = 0.4$ mm nearly corresponds to the simulated one for $s = 0.5$ mm. The error of the higher resonant frequency could be caused by the tightness of the screw to fix the back-short block. It is necessary to maintain constant tension of the

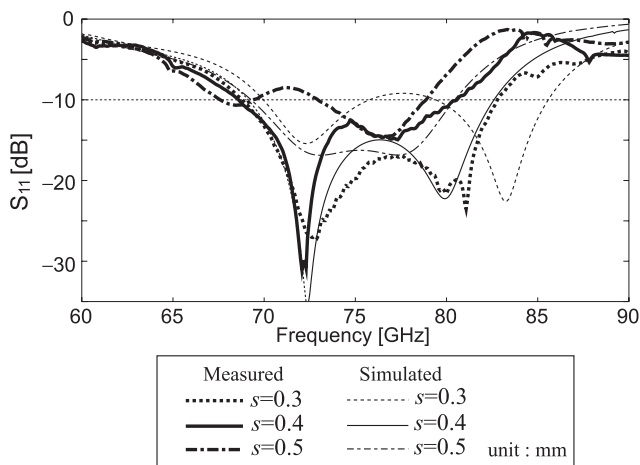


Fig. 8 Reflection S_{11} in changing back-short length s . ($h = 4.3$ mm)

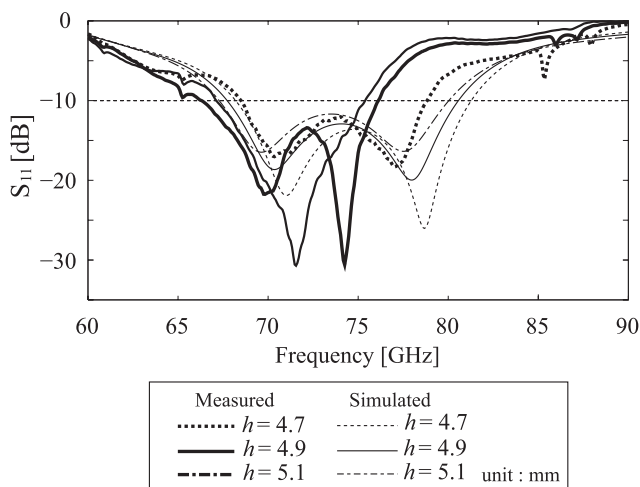


Fig. 9 Reflection S_{11} in changing length h of the radiating waveguide. ($s = 0.4$ mm)

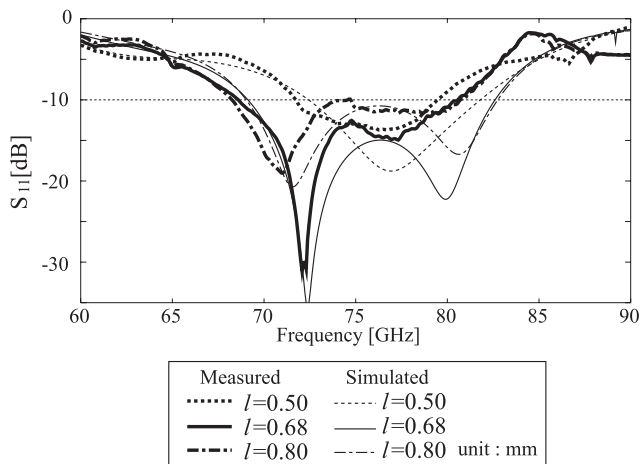


Fig. 10 Reflection S_{11} in changing the probe length l .

screw during measurement.

Figure 9 shows the reflection S_{11} when changing the length h of the radiating waveguide 4.7, 4.9, 5.1 mm, where the back-short length s is fixed in 0.4 mm. Both resonant frequencies change when h changes. In the design of the antenna, the lower resonant frequency can be controlled by changing the length h of the radiating waveguide. The shift of the higher resonant frequency is compensated by changing the length s of the back-short waveguide, afterward. Therefore, both resonant frequencies can be controlled by changing the lengths h of the radiating waveguide and s of the back-short waveguide.

Next, reflection S_{11} , when changing length l of the probe inserted into the waveguide, is shown in Fig. 10. When the length l is shorter than the optimized value 0.68 mm, the double resonance is not generated. It could be because the coupling between the electric current on the probe and the magnetic field in the waveguide is small. Moreover, when the length l is longer than the optimized value, the reflection increases. When the probe is inserted so as its tip corresponds approximately to the center of the waveguide, reflection of the antenna indicates the lowest value and performs over broad bandwidth.

3.1.2 Directivity

The simulated directive pattern is shown in Fig. 11 and summarized in Table 1. The beam width was 96 deg. in E-plane and 79.5 deg. in H-plane. The directivity in the perpendicular direction was 5.2 dBi and was the similar level with the ordinary patch antenna. When the radiating waveguide is shaped into a horn as shown in Fig. 12, the directivity increases as shown in Fig. 13 and Tabel 1. The horn structure affected the reflection characteristic S_{11} as shown in Fig. 14.

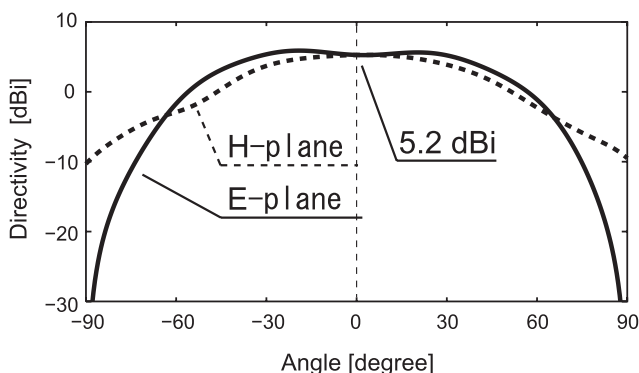


Fig. 11 Simulated directivity of the aperture antenna with metal block for back-short waveguide.

Table 1 Directivity of the aperture antenna and the horn antenna with metal block for back-short waveguide.

Waveguide	-3 dB beam width		Directivity (0 deg.)
	E-plane	H-plane	
Waveguide	96 deg.	79.5 deg.	5.2 dBi
Horn	30.5 deg.	28.0 deg.	11.7 dBi

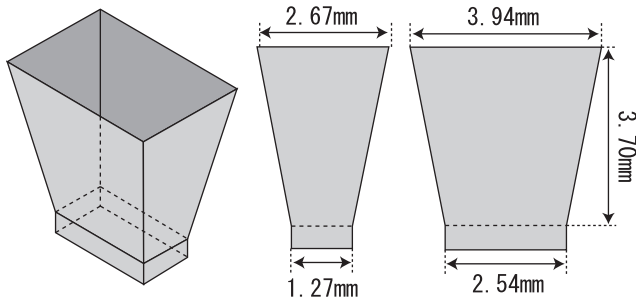


Fig. 12 Geometrical dimensions of horn shape for radiating waveguide.

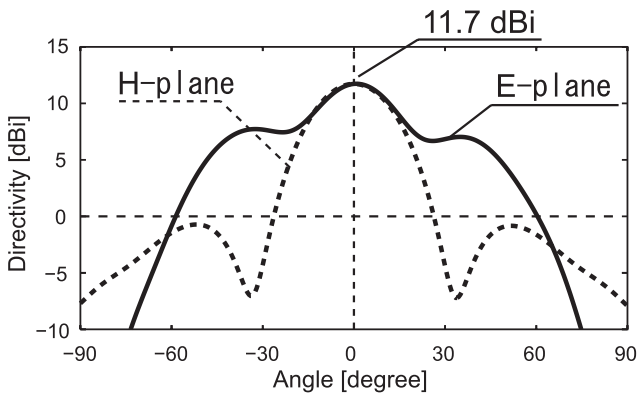


Fig. 13 Simulated directivity of the horn antenna for radiating waveguide.

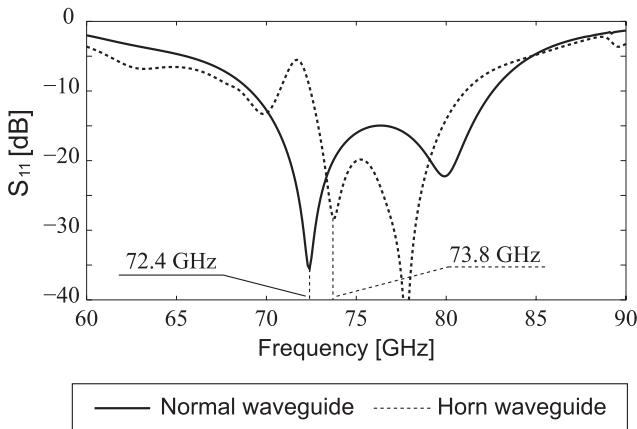


Fig. 14 Simulated reflection characteristics S_{11} of the antennas with radiating waveguide and with horn.

The directivity of perpendicular direction rises significantly and the beam width becomes narrower. The directivity can be controlled by the shape of the radiating waveguide.

3.2 Aperture Antenna with Multi-Layer LTCC Substrate

The other aperture antenna was fabricated using the multi-layer LTCC substrate. The printed pattern of the middle layer with the signal line of the antenna is shown in Fig. 15. The photographs of the fabricated antenna are shown in Fig. 16. The broad wall width a' of the quasi-waveguide

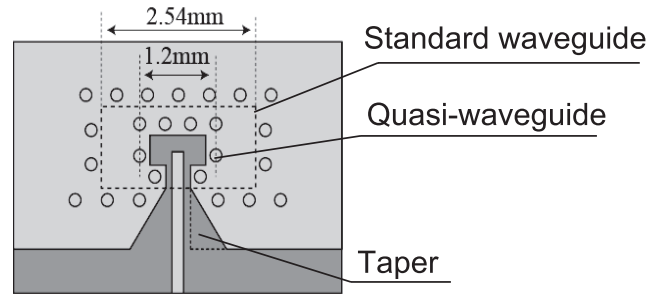


Fig. 15 Printed pattern of the middle layer with the signal line of the aperture antenna with multi-layer LTCC substrate.

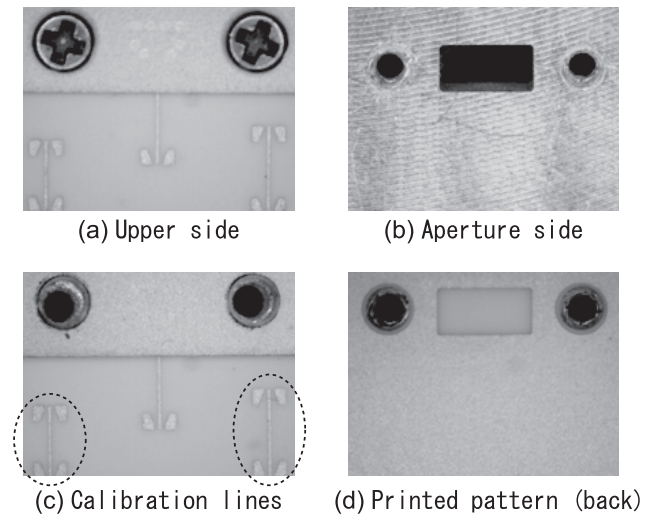


Fig. 16 Photographs of the aperture antenna with multi-layer LTCC substrate.

was 1.2 mm while that of the standard waveguide of WR-10 was 2.54 mm. The dimensions of the quasi-waveguide in the substrate were designed to be smaller than the standard one due to high relative dielectric constant of 7.1. The thickness of the substrate corresponds to the length of the back-short waveguide and was 0.28 mm chosen from the commercially supplied substrate, which was close to the optimum dimension. The calibration lines are printed on the substrate as shown in Fig. 16(c).

3.2.1 Reflection S_{11}

The measured and simulated reflections S_{11} are shown in Fig. 17. The bandwidth of the simulated reflection S_{11} lower than -10 dB was 25.7 GHz when the taper structure was applied at the feeding. Reflection level was higher when the taper structure was not applied. Almost similar reflection level with simulation was obtained by measurement.

Electric field distributions at 84.9 GHz, where reflection level is minimum, are shown in Fig. 18. Figure 18(a) shows the electric field when the size of the quasi-waveguide is the same with the hollow radiating waveguide. In this case, undesirable higher order mode is generated in the quasi-waveguide of the substrate. When the size of the

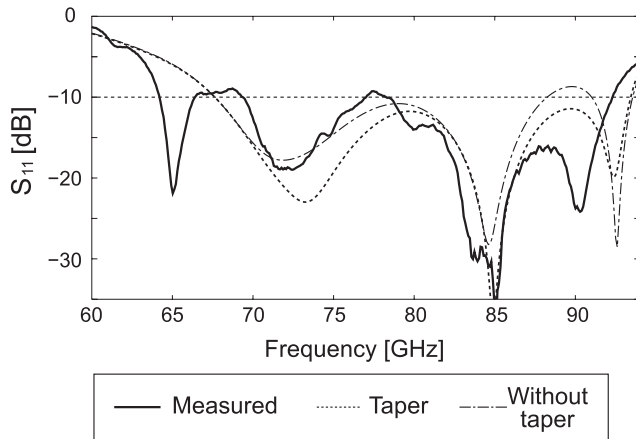


Fig. 17 Measured and simulated reflections S_{11} of the aperture antennas with multi-layer LTCC substrate.

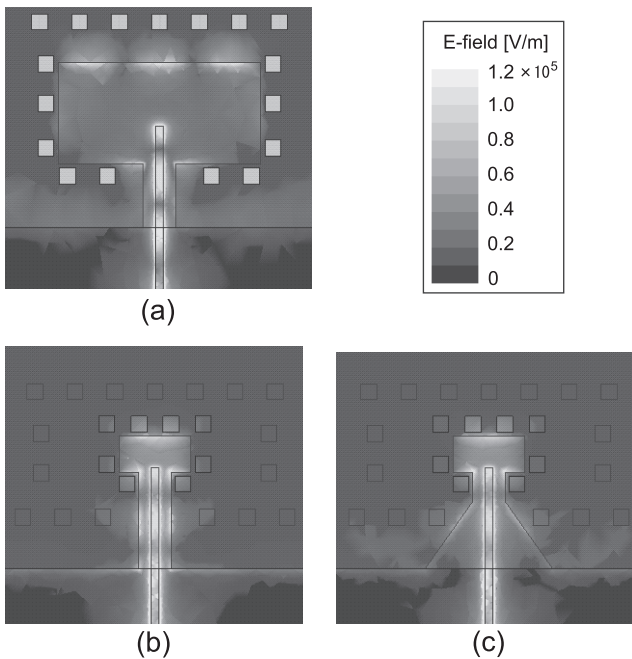


Fig. 18 Simulated electric field distributions of the aperture antennas with multi-layer LTCC substrate. (a) Width of the quasi waveguide is the same with the standard one. (b) Equivalent width of Eq. (1) is applied to the quasi waveguide without taper structure. (c) Equivalent width of Eq. (1) is applied to the quasi waveguide with taper structure.

quasi-waveguide is designed to be small, the higher order mode is not observed in the quasi-waveguide as shown in Figs. 18(b) and (c).

3.2.2 Directivity

The simulated directivity of the aperture antenna with the multi-layer substrate at 84.9 GHz is shown in Fig. 19. The peak directivity was observed in the front direction. Some degradation of directivity could be due to the leakage loss observed in the Figs. 18(b) and (c) of the electric field distribution.

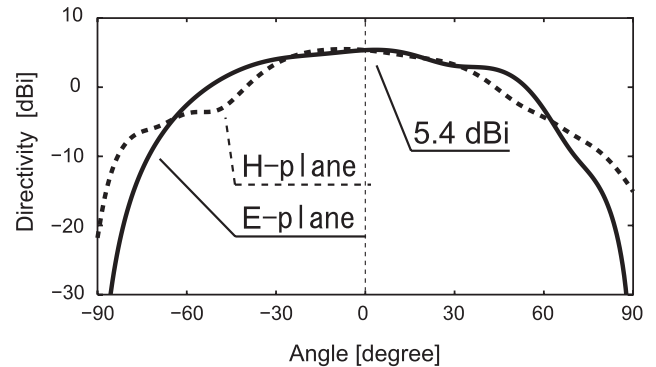


Fig. 19 Simulated directivity of the aperture antenna with multi-layer LTCC substrate.

4. Conclusion

Two types of the low-profile aperture antennas were developed to use in the millimeter-wave package. Reflection S_{11} and directivity were evaluated by simulations and measurements. The antenna with the metal block for the back-short waveguide performs the broad frequency bandwidth 12.8 GHz for S_{11} lower than -10 dB. On the other hand, the bandwidth of the antenna with multi-layer LTCC substrate for reflection lower than -10 dB is 25.7 GHz. In the design of the antenna with multi-layer substrate, the dimensions of the quasi-waveguide are designed to prevent higher order mode. Moreover, the taper structure is installed at the feeding to reduce reflection. The future study is the gain measurement and investigation of the multi-resonance for broad bandwidth.

References

- [1] C. Park and T.S. Rappaport, "Sort-range wireless communications for next generation networks: UWB, 60 GHz millimeter-wave WPAN, ZigBee," IEEE Wireless Commun. Mag., vol.14, no.4, pp.70–78, Aug. 2007.
- [2] Wireless HD, LLC, <http://www.wirelesshd.org/>
- [3] H. Shoki, Y. Tsutsumi, and S. Sekine, "Millimeter antenna technologies to realize ultra high speed wireless communication systems," IEICE Trans. Commun. (Japanese Edition), vol.J90-B, no.9, pp.810–820, Sept. 2007.
- [4] Y.P. Zhang and D. Liu, "Antenna-on-chip and antenna-in-package solutions to highly integrated millimeter-wave devices for wireless communications," IEEE Trans. Antennas Propag., vol.57, no.10, pp.2830–2841, Oct. 2009.
- [5] K.J. Lee, M. Kim, and S. Jeon, "Multi-layer dielectric cavity antennas with extended aperture height," IEICE Trans. Commun., vol.E94-B, no.2, pp.573–575, Feb. 2011.
- [6] Y. Tsutsumi, M. Nishio, S. Sekine, H. Shoki, and T. Morooka, "A triangular loop antenna mounted adjacent to a lossy semiconductor substrate for millimeter-wave WPAN," Proc. International Symposium Antennas and Propagation, pp.101–104, Niigata, Japan, Aug. 2007.
- [7] K. Li, T. Sato, J. Gao, H. Harada, and S. Kato, "Wideband planar antenna for millimeter-wave wireless personal area network," IEICE Technical Report, RCS2008-287, March 2009.
- [8] Y.P. Zhang, M. Sun, and L.H. Guo, "On-chip antennas for 60-GHz radios in silicon technology," IEEE Trans. Electron Devices, vol.52,

no.7, pp.1664–1668, July 2005.

- [9] S. Montusclat, F. Gianesello, and D. Gloria, “Silicon full integrated LNA, filter and antenna system beyond 40 GHz for MNW wireless communication links in advanced CMOS technologies,” IEEE Radio Frequency Integrated Circuits (RFIC) Symposium, San Francisco, CA, June 2006.
- [10] M. Pons, F. Touati, and P. Senn, “Study of on-chip integrated antennas using standard silicon technology for short distance communications,” The European Conference on Wireless technology 2005, vol.3, pp.253–356, Paris, France, Oct. 2005.
- [11] T. Seki, K. Nishikawa, Y. Suzuki, I. Toyoda, and K. Tsunekawa, “60 GHz monolithic LTCC module for wireless communication systems,” Proc. 36th European Microwave Conference, pp.1671–1674, Manchester, UK, Sept. 2006.
- [12] Y. Deguchi, K. Sakakibara, N. Kikuma, and H. Hirayama, “Design and optimization of millimeter-wave microstrip-to-waveguide transition operating over broad frequency bandwidth,” IEICE Trans. Electron., vol.E90-C, no.1, pp.157–164, Jan. 2007.
- [13] M. Hirono, K. Imai, K. Sakakibara, N. Kikuma, and H. Hirayama, “Measured performance of broadband microstrip-to-waveguide transition on multi-layer substrate in the millimeter-wave band,” IEICE Trans. Commun., vol.J91-B, no.9, pp.1057–1065, Sept. 2008.
- [14] T. Hirano, K. Okada, J. Hirokawa, and M. Ando, “Thru-line (TL) calibration technique for on-wafer measurement,” Proc. International Symposium on Antennas and Propagation, Macao, China, Nov. 2010.



Nobuyoshi Kikuma was born in Ishikawa, Japan, on January 7, 1960. He received the B.S. degree in electronic engineering from Nagoya Institute of Technology, Japan, in 1982, and the M.S. and Ph.D. degrees in electrical engineering from Kyoto University, Japan, in 1984 and 1987, respectively. From 1987 to 1988, he was a Research Associate at Kyoto University. In 1988 he joined Nagoya Institute of Technology, where he has been a Professor since 2001. His research interests include adaptive and signal processing array, multipath propagation analysis, mobile and indoor wireless communication, and electromagnetic field theory. He received the 4th Telecommunications Advancement Foundation Award in 1989. Dr. Kikuma is a senior member of the IEEE.



Hiroshi Hirayama received his B.E., M.E., and Ph.D. in Electrical Engineering from the University of Electro-Communications in Chofu, Japan, in 1998, 2000, and 2003, respectively. Since 2003 he has been with the Nagoya Institute of Technology, where he is currently a research associate. His research interests include signal processing techniques and EMC/EMI. Dr. Hirayama is a member of IEEE.



Shintaro Yano was born in Gifu, Japan, on September 4, 1986. He received the B.S. degree in Electrical and Electronics Engineering from Nagoya Institute of Technology, Nagoya, Japan, in 2009, and the M.S. degrees in electrical and computer engineering from Nagoya Institute of Technology, Nagoya, Japan, in 2011. He is currently working at MASPRO DENKOH Corporation, Aichi, Japan.



Kunio Sakakibara was born in Aichi, Japan, on November 8, 1968. He received the B.S. degree in Electrical and Computer Engineering from Nagoya Institute of Technology, Nagoya, Japan, in 1991, the M.S. and D.E. degrees in Electrical and Electronic Engineering from Tokyo Institute of Technology, Tokyo, Japan in 1993 and 1996, respectively. From 1996 to 2002, he worked at Toyota Central Research and Development Laboratories, Inc., Aichi, and was engaged in development of antennas for millimeter-wave automotive radar systems. From 2000 to 2001, he was with the department of Microwave Techniques in University of Ulm, Ulm, Germany, as a Guest Researcher. He was a lecturer at Nagoya Institute of Technology from 2002 to 2004, and is currently an Associate Professor. His research interest has been millimeter-wave antennas and circuits. Dr. Sakakibara is a senior member of IEEE.

From 2000 to 2001, he was with the department of Microwave Techniques in University of Ulm, Ulm, Germany, as a Guest Researcher. He was a lecturer at Nagoya Institute of Technology from 2002 to 2004, and is currently an Associate Professor. His research interest has been millimeter-wave antennas and circuits. Dr. Sakakibara is a senior member of IEEE.